J Clin Immunol (2012) 32:942–958
DOI 10.1007/s10875-012-9698-8

Clinical, Functional and Genetic Analysis of Twenty-Four Patients with Chronic Granulomatous Disease – Identification of Eight Novel Mutations in *CYBB* and *NCF2* Genes

Cécile Martel · Michelle Mollin · Sylvain Beaumel · Jean Paul Brion · Charles Coutton · Véronique Satre · Gaëlle Vieville · Mary Callanan · Christine Lefebvre · Alexandra Salmon · Anne Pagnier · Dominique Plantaz · Cécile Bost-Bru · Laurence Eitenschenck · Isabelle Durieu · Daniel Floret · Claire Galambrun · Hervé Chambost · Gérard Michel · Jean-Louis Stephan · Olivier Hermine · Stéphane Blanche · Nathalie Blot · Hervé Rubié · Guillaume Pouessel · Stephanie Drillon-Haus · Bernard Conrad · Klara M. Posfay-Barbe · Zuzana Havlicekova · Tamara Voskresenky-Baricic · Kelecic Jadranka · Maria Cristina Arriazu · Luis Alberto Garcia · Lamia Sfaihi Ben Mansour · Pierre Bordigoni · Marie José Stasia

Received: 1 February 2012 / Accepted: 10 April 2012 / Published online: 5 May 2012

Abstract Chronic granulomatous disease is an inherited disorder in which phagocytes lack a functional NADPH oxidase and cannot produce superoxide anions. The most common form is caused by mutations in *CYBB* encoding gp91*phox*. We investigated 24 CGD patients and their families. Twenty-one mutations in *CYBB* were classified as $X91^0$, $X91^+$ or $X91^-$ variants according to cytochrome b_{558} expression. Point mutations in encoding regions represented 50 % of the mutations found in *CYBB*, splice site mutations 27 %, deletions and insertions 23 %. Eight mutations in *CYBB* were novel leading to $X91^0$CGD cases. Two of these were point mutations: c493G>T and a double mutation c625C>G in exon 6 and c1510C>T in exon 12 leading to a premature stop codon at Gly165 in gp91*phox* and missense mutations His209Arg/Thr503Ile respectively. Two novel splice

Cécile Martel and Michelle Mollin contributed equally to the work

C. Martel · M. Mollin · S. Beaumel · M. J. Stasia (✉)
Chronic Granulomatous Disease Diagnosis and Research Centre (CDiReC), Pôle Biologie, CHU de Grenoble,
Grenoble 38043, France
e-mail: MJStasia@chu-grenoble.fr

S. Beaumel · M. J. Stasia
CDiReC, Therex-TIMC/Imag, UMR CNRS 5525,
UJF-Grenoble 1,
Grenoble 38041, France

J. P. Brion
Service d'infectiologie, Pôle Médecine Aigue et Communautaire,
CHU Grenoble,
Grenoble 38043, France

C. Coutton · V. Satre · G. Vieville
Laboratoire de Génétique Chromosomique, Pôle Couple/Enfants,
CHU de Grenoble,
Grenoble 38043, France

C. Coutton · V. Satre
Equipe "Génétique, Infertilité et Thérapeutiques" Laboratoire AGIM, CNRS FRE3405, La Tronche, F-38700,
Université Joseph Fourier,
Grenoble 38041, France

M. Callanan · C. Lefebvre
Laboratoire Génétique et Onco-Hematologie, Pôle Biologie,
CHU Grenoble,
Grenoble 38043, France

mutations in 5′intronic regions of introns 1 and 6 were found. A novel deletion/insertion c1024_1026delCTG/insT results in a frameshift introducing a stop codon at position 346 in gp91*phox*. The last novel mutation was the insertion of a T at c1373 leading to a frameshift and a premature stop codon at position 484 in gp91*phox*. For the first time the precise size of two large mutations in *CYBB* was determined by array-comparative genomic hybridization and carriers' status were evaluated by multiplex ligation-dependent probe amplification assay. No clear correlation between clinical severity and *CYBB* mutations could be established. Of three mutations in *CYBA, NCF1 and NCF2* leading to rare autosomal recessive CGD, one nonsense mutation c29G>A in exon 1 of *NCF2* was new.

Keywords Chronic granulomatous disease · NADPH oxidase · Nox · mutation

Introduction

Chronic granulomatous disease (CGD) is a rare genetic syndrome characterized by a dysfunction of the respiratory burst of phagocytic cells (such as neutrophils, monocytes, macrophages and eosinophils) essential to kill phagocytized pathogens. Phagocytes of CGD patients normally engulf invading bacteria but fail to kill them. Classically, CGD is diagnosed in childhood with recurrent, severe infections at epithelial surfaces or in more vital organs such as the liver, lung and brain. The incidence of this disease is between 1 in 200,000 and 1 in 250,000 cases worldwide [1]. The respiratory burst is mediated by a variety of reactive oxygen species (ROS) generated on stimulation of the membrane NADPH oxidase complex. This enzyme that produces superoxide consists of two membrane-bound subunits (gp91*phox* or Nox2 and p22*phox*) forming cytochrome b_{558} and three cytosolic proteins (p40*phox*, p47*phox* and p67*phox*) involved in the regulation of the enzyme activity. Cytochrome b_{558}, the terminal redox membrane component of the phagocyte NADPH oxidase makes the electron transfer from NADPH to FAD through two hemes [2]. About 60 % of CGD patients suffer from X linked recessive (XLR) CGD due to mutations in *CYBB* encoding gp91*phox*. In the majority of cases gp91*phox* expression is absent because of the instability of the mRNA or of the mutated protein and NADPH oxidase activity is totally abolished. This phenotype is called $X91^0$CGD. Sometimes missense mutations in *CYBB* lead to extremely rare CGD variants termed X^+ or X^-CGD and are characterized by normal or low Nox2 expression respectively and are associated with no or only faint NADPH oxidase activity [3]. The autosomal recessive forms of CGD (ARCGD) are due to mutations in *CYBA*, the gene that encodes p22*phox* in approximately 3 % of the patients, in the *NCF1* gene encoding the cytosolic protein p47*phox* (~25 %) or in the *NCF2* gene encoding the cytosolic protein p67*phox*

M. Callanan
Ontogenèse et Oncogenèse Moléculaire - Inserm U823,
Institut A. Bonniot,
UJF-Grenoble 1,
38041 Grenoble, France

A. Salmon · P. Bordigoni
Département d'Oncologie et d'Hématologie Pédiatriques et de Thérapie Cellulaire, Hôpital d'Enfants, CHU de Nancy,
54511 Vandoeuvre-Lès-Nancy, France

A. Pagnier · D. Plantaz · C. Bost-Bru
Département de Pédiatrie, Pôle Couple/Enfant, CHU de Grenoble,
Grenoble 38043, France

L. Eitenschenck
Service de Pédiatrie, Centre Hospitalier de Voiron,
Grenoble 38500, France

I. Durieu
Service de Médecine Interne et Pathologie Vasculaire,
Centre Hospitalier Lyon-Sud,
Lyon, France

D. Floret
Université Claude Bernard Lyon1- Service d'Urgences et Réanimation Pédiatrique Hôpital Femme Mère Enfant,
Bron, France

C. Galambrun · H. Chambost · G. Michel
Service de Pédiatrie et Hématologie Pédiatrique,
CHU Hôpital d'Enfants, La Timone,
Marseille 13385, France

J.-L. Stephan
Service de Pédiatrie, Hôpital Nord,
Saint-Etienne, France

O. Hermine
Service d'Hématologie Adulte, Hôpital Necker-Enfants Malades,
AP-HP,
Paris, France

S. Blanche
Unité d'Immunologie et d'Hématologie Pédiatrique,
Hôpital Necker–Enfants Malades, AP-HP,
Paris, France

N. Blot
Service de Pédiatrie Néonatologique, CH Sallanches,
Sallanches, France

H. Rubié
Service Pédiatrie - Hématologie,
Oncologie Pôle Enfants Hôpital des Enfants,
CHU de Toulouse,
31059 Toulouse, France

(~3 %). One patient has been described with mutations in *NCF4*, the gene encoding p40*phox* [4].

Very recently two articles listed all the mutations identified worldwide in the four genes involved in CGD. It confirms that CGD is a very heterogeneous genetic disease, caused by a large variety of mutations such as deletions, splice site mutations, and missense or nonsense mutations with no clear "hot-spot" location except for the *NCF1* gene [5, 6]. Clinical data from an extensive trial that included 429 European CGD patients confirmed earlier reports and showed a clear statistically significant difference in lifespan between the two main types of CGD. Indeed ARCGD was diagnosed later in life and the mean survival time was significantly better in AR patients (49.6 years) than in XL CGD (37.8 years), suggesting a milder disease course in AR patients. There appears to be a crucial need for cytochrome b_{558}, the redox center of the NADPH oxidase, while the cytosolic factors p47*phox*, p67*phox* and p40*phox* are not absolutely required for maintaining a minimal level of activity [7]. Moreover, a recent review highlighted that survival in CGD is associated with residual ROS production, independent of the mutation [8]. Indeed residual oxidase activity is often found in the most frequent AR47^{0}CGD form which displays often mild clinical expression.

In the present study, we investigated 24 patients suffering from CGD vis-à-vis NADPH oxidase activity in their phagocytes and those from their relatives. Twenty-one mutations in *CYBB* were detected; three led to rare X$^+$CGD and X$^-$CGD variants and seven were novel. Three cases of rare ARCGD were also identified with mutations in *NCF1*, *CYBA* and *NCF2*. One nonsense mutation found in exon 1 of *NCF2* was new. Clinical severity was analyzed according to the type of mutations in *CYBB*.

Materials and Methods

Patients

Patients from France, Slovakia, Croatia, Switzerland, Tunisia and Argentina were diagnosed as having CGD on the basis of their clinical history, examination and the inability of their phagocytes to generate superoxide anions detectable by SOD sensitive cytochrome *c* reduction assay, resorufine fluorescence measurement (Amplex® Red Hydrogen Peroxide/Peroxidase Assay Kit, Invitrogen Life technologies, Villebon sur Yvette, France) or nitroblue tetrazolium dye reduction (NBT) slide test [9]. XCGD and ARCGD classifications were made according to pedigree analysis, western-blotting results, the identification of maternal carrier status and gene analysis. The results of the mosaic pattern by NBT assay from the mothers' peripheral neutrophils were consistent with an X-linked inheritance. XCGD subtypes were determined according to the nomenclature X91^0, X91$^-$, X91$^+$ where the superscript denotes whether the level of gp91*phox* is undetectable (^{0}), low ($^-$) or normal ($^+$) as determined by immunoblot analysis and/or spectral analysis. A summary of the clinical history of the patients is given in Table I. Blood samples were collected from healthy volunteers, patients and relatives after obtaining their signed informed consent. Written consent for DNA analysis of samples from patients, parents and relatives was also obtained.

Cell Preparations

Human neutrophils and mononuclear cells (lymphocytes plus monocytes) were isolated from 25 ml of citrated blood from patients, their parents, and healthy volunteers as

G. Pouessel
Service de Pédiatrie, CH de Roubaix,
Roubaix, France

S. Drillon-Haus
Service de Pédiatrie et Onco-hématologie, Hôpital de Hautepierre,
CHU Strasbourg,
Strasbourg, France

B. Conrad
DiaGena, MCL Niederwangen,
Niederwangen, Koniz, Switzerland

K. M. Posfay-Barbe
Pediatric Infectious Diseases, Children's Hospital, University Hospital of Geneva,
Geneva, Switzerland

Z. Havlicekova
Department of Pediatrics, Center of Experimental and Clinical Respirology II, Comenius University,
Jessenius School of Medicine,
Martin, Slovakia

T. Voskresenky-Baricic
Pediatric Clinic Klaiceva,
Clinical Hospital Center Sestre milosrdnice Zagreb,
Zagreb, Croatia

K. Jadranka
Department of Pediatrics, University Hospital Center Zagreb,
Zagreb, Croatia

M. C. Arriazu · L. A. Garcia
Department of Pediatric and Pneumology,
Hospital Privado Comunidad,
Mar del Plata, Argentina

L. S. B. Mansour
Service de pédiatrie, CHU Hédi Chaker,
Sfax, Tunisia

Table I Summary of clinical history of CGD patients

	CGD type	Date of Birth	Age of diagnosis	Severe infections	Minor infections	Treatment
P1	$X91^0$	12/26/03	3 years	Lung granuloma (fungi)	Chronic pneumonia, recurrent adenopathies (*S. aureus*) post BCG, fungal skin abcesses	Prophylactic[a] Interferon γ
P2	$X91^0$	06/22/89	3 years	Liver abcesses (*S. aureus*), sepsis (*Salmonella*)	Granuloma in intestinal tract	Successful Allogeneic BMT (10/09)
P3	$X91^0$	09/01/09	17 months	Purulent pericarditis	Pneumonia, Pyodermia, Becegitis, axillary lymphadenitis, acute entero-colitis, Intestinal obstruction caused by granulomatous inflammation	Prophylactic[a] Steroids, MUD HSCT (01/12)
P4	$X91^0$	01/23/07	11 months	Liver, splenic, pulmonary abscesses, sepsis (*Burkhoderia cepaciae*), macrophagic activation syndrome	Cutaneous abcess, pyodermitis, Gastroenteritis, pulmonary infection (fungi)	Successful Allogeneic BMT (12/08)
P5	$X91^0$	02/27/07	3 months	Multifocal pulmonary infections (*A. fumigatus*)		Successful Allogeneic BMT (03/08)
P7	$X91^0$	03/13/09	2 months	Sepsis (*E. Coli*)	Pneumopathy	Prophylactic[a]
P8	$X91^0$	12/19/98	6 years	Liver and spleen abcesses	Reccurent pulmonary infections, Vomiting gastro-intestinal troubles	Prophylactic[a]
P9	$X91^0$	04/05/05	2 years	Pulmonary granuloma	Mouth candidosis, Recurrent cervical adenopathies, Sus collarbonary abcesses (*St. aureus*), chronic cough	Prophylactic[a]
P10	$X91^0$	12/29/93 DCD[b]	18 months	Severe pulmonary aspergillosis	Pneumonia, Reccurent skin infections (*S. aureus*), colitis, diarrhea, stenosis,	Amphotericine B, Caspofungine Allogeneic BMT (07/07)
P11	$X91^0$	01/30/09	4 months		Recurrent skin infections, furonculosis, perianal fissures (*K. oxytoca*), oesophagitis granuloma	Prophylactic[a]
P12	$X91^0$	01/03/03	4 years	Liver; spleen and bone granuloma	Pneumonia, Purulent infections	Prophylactic[a] Interferon γ Allogeneic BMT (07/07)
P13	$X91^0$	07/21/92	3 years	Pulmonary aspergillosis	Pustular skin lesions, colitis, diarrhea	Prophylactic[a]
P14	$X91^-$	03/17/05	5 years		Pneumonia, Skin abcesses, granuloma in the intestinal tract	Prophylactic[a]
P15	$X91^+$	12/19/03	6 years	Pulmonary abscess, sepsis, hyperthermia	Becegitis, Colitis, Perianal abscess, recurrent adenopathies, diarrhea	Prophylactic[a]

Table I (continued)

	CGD type	Date of Birth	Age of diagnosis	Severe infections	Minor infections	Treatment
P16	$X91^{+}$	07/13/04	18 months		Reccurent adenopathies (*S. aureus*), skin infections	Prophylactic[a]
P17	$X91^{0}$	01/05/11	2 months	Pulmonary aspergillosis	Anemia, splenomegaly, inflammatory syndromes, retroperitoneal adenopathies	Ceftriaxone, meropenem, teicoplanin caspofungine
P18	$X91^{0}$	04/27/79	2 years		Pneumonia, emphysema, adenopathies, skin abcesses, splenomegaly, acnea	Prophylactic[a]
P19	$X91^{0}$	06/05/02	6 years		Bronchopneumonia, Recurrent skin abcesses (*St. aureus*), pulmonary nodules	Prophylactic[a]
P20	$X91^{0}$	08/11/05	1 year	Sepsis, Pulmonary abcess with lobectomy	Mac Leod syndrome	Prophylactic[a]
P21	$X91^{0}$	11/05/86	2 years	Pulmonary aspergillosis, osteomyelitis, liver granuloma	Recurrent skin abcesses, anal and splenic abcesses, otitis media, Mac Leod syndrome	Prophylactic[a] Interferon γ from 1994 to 2005
P22	$AR67^{0}$	08/05/08	3 months	Splenic abscesses	Respiratory tract infections, Bronchopneumonia	Prophylactic[a]
P23	$AR22^{0}$	03/25/07 DCD[c]	13 months	Severe Pulmonary aspergillosis, osteomyelitis, hydrocephalus	Axillary and cervical adenopathies, becegitis, retropharingus abces (*K. pneumoniae*), recurrent skin abscesses, chronic cough	Amoxicilline, Fosfomycine, Amphotericine B, Variconazole Prophylactic[a]
P24	$AR47^{0}$	08/03/03	7 years	Sepsis, Coronary vasculitis (Kawasaki syndrome), pulmonary granuloma	Adenoïdectomy, Impetigo, Molluscum contagiosum, Rhinopharyngitis, Colitis, recurrent perianal abcesses (*Streptococcus B*), diarrhea Diffuse erythematous rash	Acetylsalicylic acid, corticoids, Infliximab, Methotrexate, vancomycin, ciprofloxacine, amykacine and immunoglobulins Prophylactic[a]

The numbers in the first column designate the CGD patients studied in this work. The CGD type and subtypes was determined as described in "Material and Methods". Patients exhibiting new mutations are underlined. [a] Trimethoprim-sulfamethoxazole and itraconazole. [b] Death secondary to "inflammatory flare-ups" after bone marrow transplantation. [c] Death secondary to severe aspergillosis in lung, bone and brain refractory to treatment. MUD HSCT; Matched Unrelated Donor Human Stem Cell Transplantation. All were index cases except P5

described [10]. Lymphocytes purified by Ficoll-Hypaque density gradient centrifugation were infected with the B95-8 strain of EBV and cultured, as previously described [11].

Measurement of NADPH Oxidase Activity in Neutrophils

ROS production by stimulated neutrophils from the patients, their relatives and healthy donors was measured using several approaches depending on the age and amount of the blood sampled. For each diagnosis, a control of fresh blood and a control blood sample that had been transported under identical conditions to the patient's blood sample were included in the activity determination. The phagocytic capacity and ROS production of the neutrophils were assessed with the NBT reduction test after opsonized latex bead or PMA activation. NADPH oxidase activity of intact neutrophils was also assessed by measuring the rate of superoxide-sensitive cytochrome *c* reduction in presence of SOD (ε_{550nm}= 21.1 $mM^{-1}.cm^{-1}$) [12]. Simultaneous assessment of Nox2 protein expression and oxidase activity was performed by flow cytometry. Briefly, purified neutrophils were incubated with mAb 7D5 (Ref D162-3, Clinisciences, Nanterre, France) directed against an external epitope of Nox2 or an irrelevant monoclonal IgG1 and then incubated with Alexa Fluor 633 goat-F(ab′)2 fragment anti-mouse IgG1 (H+L). Next, the cells were incubated 10 min at 37°C with 0.5 μM dihydrorhodamine (DHR), then activated with 80 ng/ml PMA for 15 min at 37°C. Finally, the cells were kept on ice until flow cytometry analysis (FACScalibur, Becton Dickinson, Le Pont de Claix, France). Data were collected from 10,000 events and analysed using CellQuest software (BD PharMingen). All experiments were done in triplicate [13]. Measurement of H_2O_2 production by NADPH oxidase was performed by resorufine fluorescence kinetics [14]. Human neutrophils (5×10^4 cells/well in a 96-well plate) in PBS containing 0.9 mM $CaCl_2$, 0.5 mM $MgCl_2$, 20 mM glucose, 50 μM Resorufine, and 10 U/ml HRPO were stimulated at 37°C with 10 ng/ml PMA. The rate of fluorescence of resorufine oxidation was recorded at 590 nm every 30 s for 15 min in a fluorometer (Twinkle LB 970 Berthold SA, Thoiry, France) connected to a computer. Fluorescence values at 10 min after activation were registered and reported to a calibration curve made with increasing amount of H_2O_2. The results were expressed as μmoles of H_2O_2 produced/min/10^6 neutrophils.

Cytochrome b_{558} Spectroscopy

Purified neutrophils treated with 3 mM diisopropyl fluorophosphate were lysed with 1 % Triton X100 (v/v) for cytochrome b_{558} extraction. The supernatant was used for immunoblotting and cytochrome b_{558} spectroscopy. Reduced minus oxidized differential absorption spectra were recorded as described in [15].

SDS-PAGE and Immunoblotting

Solubilized proteins were run on SDS-PAGE [16], electrotransferred to nitrocellulose [17] and immunodetected by monoclonal antibodies mAbs 449 and 48 directed against p22*phox* and gp91*phox*, respectively [18], or by rabbit polyclonal antipeptide antibodies directed against p47*phox* [19] and by goat polyclonal antipeptide antibodies against p67*phox* (Ref SC 7662, Santa Cruz Biotechnology Inc. CA, USA).

Preparation of RNA and DNA

Total RNA was isolated from either mononuclear cells or EBV-transformed B lymphocytes of both CGD patients and healthy individuals, using a modified single-step method [20]. Genomic DNA was purified with a purification kit (ref A1120 Wizard^R genomic DNA, Promega Biosciences inc. CA, USA).

cDNA Amplification

First-strand cDNA was synthesized from total RNA by reverse transcriptase reaction according to the manufacturer's instructions (QBiogen, Montréal, Canada). Total cDNAs were immediately amplified by PCR, in three to four overlapping fragments and analysed on agarose gel [20]. The bands were photographed under UV (GelDoc XR+Biorad, Marnes-la-Coquette, France). In some cases PCR products were purified from agarose gel with the Sephaglass kit (Amersham Pharmacia, Orsay, France). All PCR products were sequenced (Eurofins MWG Operon, Ebersberg, Germany) using an ABI 3730 XL 96 capillary sequencer (Perkin Elmer, Foster City, CA, USA). More than 200 sequences of cDNA prepared from the controls' mRNA, of gp91*phox*, p22*phox*, p47*phox* and p67*phox* were analyzed to rule out the possibility of polymorphisms.

Genomic DNA Amplification

To identify the genetic defect, exon sequences plus the intron flanking regions of *CYBB*, *CYBA*, *NCF1* and *NCF2* from genomic DNA were amplified by PCR using appropriate forward and backward primers [20], followed by direct sequencing (Eurofins MWG Operon, Ebersberg, Germany). This was done for patients P1 to P18 and P22 to P24.

Gene-Scan Method for Determination of the Ratio of *NCF1* and Φ*NCF1* Genes

Fragments of genomic DNA from AR47^{0}CGD patients and their relatives were amplified by PCR with primers that anneal to regions in *NCF1* as well as to regions of Φ*NCF1* around the GTGT sequence at the start of exon 2. The ratio between the number of *NCF1* and Φ*NCF1* genes was determined [21].

Fluorescence In Situ Hybridization (FISH)

Cytogenetic analysis was performed on a cell suspension obtained after 17-hour unstimulated culture using R-banded metaphase chromosomes. Fluorescence In Situ Hybridization (FISH) studies were performed on the same cytogenetic pellet, using a mix of a control probe (CEPX, Cytocell, Amplitech) with a locus specific bacterial artificial chromosome (BAC) clone. BAC clones were selected from the UCSC genome browsers (genome.ucsc.edu/) The Xp21 BAC probes used in the study were as follows: RP11-777A16 and RP11-641C23 overlapping the *CYBB* gene and RP11-12J5 centromeric to *CYBB*. For FISH, BACs were directly labeled using a nick translation kit (Vysis, Abbott Molecular, Rungis, France), according to the manufacturer's instructions. BAC probes were denatured for 10 min at 73°C and slides were incubated for 20 h at 37°C. The post-hybridization washes were performed according to the manufacturer's instructions (Vysis kit, Abbott Molecular, Rungis, France). Slides were counterstained with DAPI/Vectashield (Vector Laboratories, Peterborough, United Kingdom). FISH signals were captured with a fluorescence microscope (M1, Carl Zeiss S.A.S. Le Pecq, France) equipped with appropriate filters, a charge-coupled device camera, and the FISH imaging software (Isis, Metasystems, Altlussheim, Germany). Twenty metaphases were analysed per slide.

Array-Comparative Genomic Hybridization (CGH-Array)

Array CGH was performed using an 180,000-oligonucleotide microarray (Human Genome CGH-Microarray Kit 180K, Agilent Technologies, Santa Clara, CA). The average spacing of the probes was 13 kb. DNA from the patient was compared with DNA from two other patients with different diseases, according to the loop model [22]. Genomic Workbench software, standard edition 6.5 (Agilent) was used to interpret the results with the following parameters: aberration algorithm ADM-2, threshold 6.0, fuzzy zero, centralisation and moving average window 0.5 Mb and 1 Mb. A copy number variation (CNV) was noted if at least three contiguous oligonucleotides showed an abnormal log2 ratio (>+0.5 or <−0.5 according the Alexa 5 deviation, red curve) with a mirror image. The Database of Genomic Variants (DGV, http://projects.tcag.ca/variation/) was used to compare findings to previously reported studies. Coordinates of CNVs are based on the UCSC GRCh37/hg19 assembly.

MLPA Analysis

A home-made MLPA kit was used to assess the carrier status of the mothers of patients P19 and P20. The design of the MLPA probes, MLPA reaction and data analysis were performed according to the recommendations of the MRC-Holland synthetic protocol (www.mlpa.com). For this study, one synthetic custom MLPA probe specific for the *CYBB* gene, comprising the two deletions, was designed. The *CYBB* specific MLPA probe spans 37,548,196 to 37,548,261 according to the human genome version GRCh37/hg19. In addition, four MLPA control probes specific to the *OCRL1* gene were included serving as controls for a proper copy number quantification. Information about sequences and ligation sites of these control probes can be obtained [23]. As the *CYBB* gene is located on the X chromosome, a heterozygous deletion will theoretically result in a 50 % reduction in female carriers.

Protein Determination

The protein content was measured using the Bradford assay [24].

Results

In this study, 21 out of 24 CGD patients (P1 to P21) presented with XCGD with a molecular defect in the *CYBB* gene. The 3 remaining patients (P22 to P24) were analysed for mutations in the *NCF2*, *CYBA* and *NCF1* genes supporting ARCGD (Table I). The criteria of severity were defined according to the type and the location of infections associated with sepsis, age at diagnosis and the presence of granuloma in vital organs. As seen in Table I, age at CGD diagnosis was between 2 months and 7 years. Most of the XCGD cases were detected early, i.e. before 4 years of age (16/21). All were index cases except patient P5 who had a younger brother previously diagnosed in another lab, and underwent bone marrow transplantation. Fourteen of the 21 XCGD patients had at least one severe infection with the presence or not of granuloma in deep organs. Five of them suffered from sepsis (P2, P4, P7, P15, P20). The main affected organs were the lung (12/21) and the liver (5/21). Five XCGD patients (P11, P14, P16, P18 and P19) only had minor infections such as subcutaneous abscess formation or in organs of the mononuclear phagocyte system, pneumonia, infections and granuloma in hollow organs (mainly gastrointestinal tract), or recurrent adenopathies. Four patients (P8, P14, P15 and P19) were diagnosed after 4 years of age and two of them had mild clinical presentation of the disease (P14, P19) (Table I). The clinical profile of $X91^{+}$CGD patients varied (P15, P16) (Table I). Five severe $X91^{0}$CGD cases (P2, P4, P5, P10 and P12) underwent allogenic bone marrow transplantation (BMT). Four of them were definitively cured (P2, P4, P5 and P12) but one patient died following an inflammatory flare up (P10). Recently patient P3 has undergone Matched Unrelated Donor Human Stem Cell Transplantation (MUD HSCT) with, to date, no

serious complication occurring. Surprisingly patient P4 presented with repeated lymphohistiocytic activation syndromes probably caused by chromosomal integration of the HHV-6 genome [25]. Regarding ARCGD cases (P22 to P24), two patients with mutations in *CYBA* and *NCF2* were diagnosed early and demonstrated a severe clinical profile (P22 and P23). On the contrary the AR47^{0}CGD case (P24) had a milder clinical profile except that he developed coronary vascularitis. Indeed at the age of 7 years (which is late for CGD diagnosis) the first clinical symptoms in this patient were recurrent perianal abcesses with chronic purulent seepage. Then, 3 months later he was hospitalized with sepsis and a diffuse erythematous and cutaneous rash. Secondary to this he had arterial hypotension treated with noradrenalin. Five days later he developed coronary vasculitis, an unusual event for CGD patients, with clinical presentation and a cardiac echography compatible with Kawasaki's syndrome. Clinical improvement was obtained with vancomycin, ciprofloxacine, amykacine and immunoglobulin treatment (Table I). Several examinations of tissues from patients (P1, P2, P9, P11, P12, P14, P21, and P24) typically showed granuloma mostly in vital organs. Prophylactic antibiotic therapy (trimethoprim/sulfamethoxazole) was always initiated. In three cases, interferon-γ was used as treatment during a short period (P1, P12 and P21). Itraconazole or other anti-fungals were given to prevent or cure pulmonary aspergillosis. Today, most patients are in stable condition with prophylactic treatments (Trimethoprim-sulfamethoxazole, and antifungal) and are under constant care and follow-up in specialized medical centers.

The NADPH oxidase activity of purified neutrophils from the 18 XCGD patients studied was totally abolished after PMA stimulation using different methods (Table II). In one X$^-$CGD patient (P14) we found a slight NADPH oxidase activity in most of the purified neutrophils by the NBT reduction test and by DHR flow cytometry (data not shown). In three patients (P1, P3 and P23) this activity could not be measured because no blood samples were available, only genomic DNA, or because blood samples were more than 48 h old when they arrived in the lab from other countries. Intermediate values were obtained in neutrophils from the mothers of all XCGD patients, except for patients P9, P17 and P20 (Table II). P6 was a 17 year-old girl followed by a pediatric hematological clinic for generalized lymphadenopathy (axillar, submadibular, intraperitoneal, and inguinal) with a non-specified granulomatous process in the lungs (first suspected to be sarcoidosis), and mild hypogamma globulinemia. She was a XCGD carrier because she had two populations of neutrophils: 30 % could not reduce NBT whereas 70 % had normal oxidase activity (Table II). Her carrier status was confirmed by genetic analysis (see below). The activation of neutrophils from the fathers of XCGD patients was always normal and comparable to neutrophil control values (data not shown). The carrier status of relatives (siblings, aunt, grand-mother) of XCGD patients was suspected from the functional and biochemical diagnosis (oxidase activity, differential spectrophotometry), but was always confirmed by the genetic analysis (Table II). The presence of cytochrome b_{558} was normal in P15 and P16 confirming that these two patients had X$^+$CGD whereas for P14 only a faint amount of cytochrome b_{558} was detected in his neutrophils by westernblot confirming the X$^-$CGD type (data not shown). Finally, NADPH oxidase activity was totally abolished in AR67^{0}CGD neutrophils except in the AR47^{0}CGD case where faint NADPH oxidase activity could be measured. In ARCGD cases the oxidase activity of both parents was normal and the carrier status was determined after genetic analysis (Table II).

Consequently, molecular genetic studies were conducted with the objective of looking for mutations in the *CYBB*, *CYBA*, *NCF1* and *NCF2* genes in affected patients and their relatives. The localization of small mutations was found from sequencing of cDNA amplified in two to four overlapping fragments (depending of the size of the cDNA) after RT-PCR using specific primers (P1 to P24, except for P20 and P21). To verify the location of mutations in the genes, mutated exonic and/or intronic regions were amplified using primers as described in Material and Methods. In the case of large mutations (P20, P21) FISH, MPLA or CGH-arrays were used to determine the size and position of the deletion.

Point mutations (missense and nonsense) in encoding regions represented 50 % of the mutations found in *CYBB* (P4, P5, P6*, P7, P8, P10, P11, P14, P15, P16), splice site mutations 29 % (P1, P2, P3, P9, P12, P18), small deletions or insertions with frameshifts 9 % (P13, P17) and large deletions 14 % (P19, P20, P21). Of the 21 mutations found in *CYBB*, 14 were previously published (for references see the review of the third update of X-linked mutations of CGD published in 2010 [6]). Mutations in the encoding region of *CYBB* were distributed along the entire sequence of gp91*phox* (Fig. 1). Seven novel mutations were found in *CYBB*, evidence of X91^{0}CGD sub-types (P1, P6*, P7, P9, P13, P17 in Table II). Two of these were splice site mutations (P1 and P9). The first one caused by a point mutation and a one base deletion in intron 1 (c45+3A>T+5delG) leading to the absence of gp91*phox* mRNA synthesis (P1). The second one was a four base deletion (c674+4delAGTG) at the beginning of intron 6 leading to exon 6 being skipped in the corresponding mRNA (P9). Two other new mutations were point mutations: one was a nonsense mutation in exon 6 (c493G>T) introducing a stop codon at Gly 165 (P6*) and the second was a double mutation c625C>G in exon 6 and c1510C>T in exon 12 leading to missense mutations Thr208Arg and Thr503Ile respectively in gp91*phox* (P7). The last two novel mutations in patients P13 and P17 (Table II) were a small deletion/insertion or insertion

Table II Phenotype and genotype of X and AR CGD patients and their relatives

	Cytc Red O_2^- nmol/min/10^6cells	Resorufine H_2O_2 µmol/min/10^6cells	NBT reduction test % positive cells	Cyt b_{558} pmol/mg	Mutations cDNA	Genomic DNA Location	Gp91*phox* Protein	CGD type Status
P1	ND	ND	ND	ND	c45+3A>T+5delG Skip exon 1 ?	Intron 1	p.Met1_Ile15del Absent	$X91^0$
M1	ND	ND	ND	ND				Carrier
S	ND	ND	ND	ND				Not carrier
P2	0	0	0	0	c46-1 G>T Skip exon 2	Intron 1	p.Leu16_Gly47del Absent	$X91^0$
M	2.7	5.1±1.7	20	18				Carrier
P3	ND	ND	ND	ND	c141+1 G>A Skip exon 2	Intron 2	p.Leu16_Gly47del Absent	$X91^0$
M	ND	ND	ND	ND				Carrier
P4	0	0	0	0	c143C>G	Exon 3	Ser48X Absent	$X91^0$
M	8.9±1.2	7,6±0,9	54	206				Carrier
Gm	ND	ND	ND	ND				Not carrier
P5	ND	0	ND	ND	c469C>T Skip exon 5	Exon 5	Arg157X Absent	$X91^0$
M	ND	10.1±0.4	ND	ND				Carrier
Au	ND	ND	ND	ND				Carrier
P6[a]	ND	21.0±2.0	69	ND	c493G>T	Exon 6	Gly165 X	Carrier X91
P7	0	0	0	0	c625C>G and c1510C>T	Exon 6 Exon 12	His209Asp and Thr503Ile Absent	$X91^0$
M	5.5	10.4±1.5	39	76				Carrier
P8	0	ND	0	0	c625C>T	Exon 6	His209Tyr Absent	$X91^0$
M	4.0±1.2	ND	36	92				Carrier
Gm	12.4±0.9	ND	96	190				Not carrier
Au	16.2±1.8	ND	84	240				Not carrier
Au	15.4±1.7	ND	92	175				Not carrier
P9	0	0	0	0	c674+4delAGTG Skip exon 6	Intron 6	p.Asn162_Glu225del Absent	$X91^0$
M	9.2±0.8	27.2±3.4	81	248				Not carrier
P10	ND	0	0	ND	c691C>T	Exon 7	Gln231X Absent	$X91^0$
M	ND	18.1±1.1	47	ND				Carrier
P11	0	ND	0	0	c752G>A	Exon 7	Trp251X Absent	$X91^0$
M	2.2±0.1	ND	30	58				Carrier
Au	17.5±0.9	ND	90	ND				Not carrier
Au	12.4±1.7	ND	78	ND				Not carrier
P12	0	ND	ND	0	C897+1 G>A Skip exon 8	Intron 8	p.Thr269_Lys299del Absent	$X91^0$
M	6.0±0.7	ND	ND	91				Carrier
P13	0	0	0	0	c1024_1026delCTG/insT	Exon 9	p.Leu342TyrfsX3 Absent	$X91^0$
M	5.5	13.8±0.4	44	109				Carrier
P14	ND	0	2[b]	0	c.1076 G>C	Exon 9	Gly359Ala Decrease	$X91^-$
M	ND	6.1±0.3	30	57				Carrier
P15	0	0	0	265	c1222G>A	Exon 10	p.Gly408Arg Present	$X91^+$
M	14.9±0.4	14.4±0.4	88	200				Carrier

Table II (continued)

	Cytc Red O_2^- nmol/min/10^6cells	Resorufine H_2O_2 µmol/min/10^6cells	NBT reduction test % positive cells	Cyt b_{558} pmol/mg	Mutations cDNA	Genomic DNA Location	Gp91*phox* Protein	CGD type Status
P16	0	ND	0	105	c1244C>T	Exon 10	p.Pro415Leu Present	$X91^+$
M	2.8±0.2	ND	50	117				Carrier
P17[c]	ND	0	0	ND	c1373insT	Exon 11	p.Gln459AlafsX26 Absent	$X91^0$
M	ND	25.8±2.8	90	ND				Not carrier
P18	0	ND	0	0	C1461+1 G>A Skip exon 11	Intron 11	p.Ile439_Gln487del Absent	$X91^0$
M	5.9±0.2	ND	50	105				Carrier
Si	5.2±0.3	ND	70	74				Carrier
Au	14.1±0.5	ND	87	180				Not carrier
P19	0	0	5	0	8,494 bp del intron 6_exon 11	Exon7_11	Absent	$X91^0$
M	4.0	8.2±1.2	33	50				Carrier
P20	0	ND	0	0	Large deletion	*CYBB*	Absent	$X91^0$
M	10.0±0.5	ND	ND	167	Around 210 kb	XK		Not Carrier
Br (tw)	14.7±0.3	ND	92	ND				Not carrier
P21	0	ND	1	0	Large deletion	*CYBB*	Absent	$X91^0$
M	6.7	ND	48	180	Around 1,3 Mb	XK		Carrier
Si	10.3	ND	90	270				Not carrier
P22	0	0	6	ND	c29G>A	Exon 1	p.Trp10X Absent	$AR67^0$
M	12.6	ND	ND	ND		*NCF2*		Carrier
F	ND	49±2.5	92	ND				Carrier
Si	ND	ND	ND	ND				Not carrier
P23	ND	ND	ND		c295_301delGTGCCCG	Exon 5 *CYBA*	p.Val99ProfsX90 Absent	$AR22^0$
M	ND	ND	ND					Carrier
P24	ND	3	6	ND	C75_76delGT	Exon 2 *NCF1*	p.Tyr26HisProfsX26 Absent	$AR47^0$
M	ND	33.6±4.2	100	ND				Carrier
F	ND	35.9±2.4	98	ND				Carrier
Br1	ND	34.9±1.3	ND	ND				Carrier
Br2	ND	38.5±3.0	ND	ND				Not carrier
Si	ND	39.7±4.2	ND	ND				Not carrier
C (n=100)	11.3±3.3	25.7±10.3	90±6	166±30	/	/	/	/

NADPH oxidase activity of patient neutrophils was determined by superoxide dismutase-inhibitable cytochrome *c* reduction assay, oxidation of Amplex Red® by fluorescence or NBT reduction slide test, as described in Materials and Methods. Protein level determination was determined by westernblotting or differential spectrophotometry (cytb_{558}) as described in "Material and Methods". Control data represent the mean ± SD (n=100). P, patient; M, mother; F, father; Gm, maternal grand-mother Br, brother; Si, sister; Au, aunt; tw, twin. [a] is for a new mutation found only in a carrier. Patients exhibiting new mutations are underlined. [b] 98% of the neutrophils of this patient demonstrated a faint oxidase activity by NBT reduction test and DHR flow cytometry.[c] Simultaneous assessment of Nox2 protein expression and oxidase activity was performed by flow cytometry as described in Material and Methods. 56 % of his mother's neutrophils showed the same faint oxidase activity. The nucleotide numbering system we have used is based on the cDNA sequence and follows the convention that +1 is the A of the ATG initiator codon as specified in [5, 6]. The notation of the mutations follows the recommendations of the human Genome Variation Society [46] (see also www.hgvs.org/mutnomen). The consequences of the mutations for protein composition have been checked with ExPASy program (http://web.expasy.org/translate/). References and accession numbers of other cases of known mutations can be found in [5, 6]

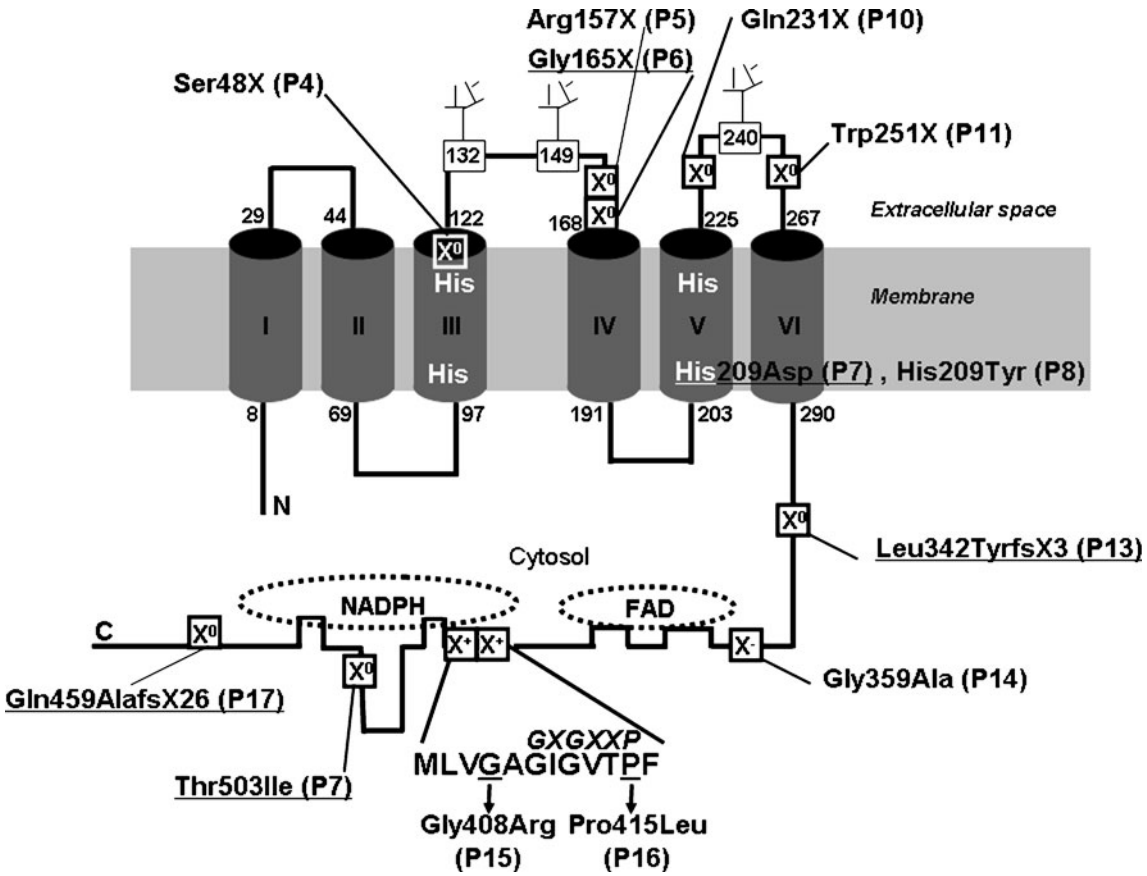

Fig. 1 Localization of point mutations in the encoding region of *CYBB* causing X91^0, X91$^-$ and X91$^+$ forms of CGD, on membrane-spanning models of gp91*phox* protein. The figure shows the location of the studied mutations leading to different sub-types of X-linked CGD in the putative organization of the polypeptide chain of gp91*phox*. Novel human mutations are underlined. The position of glycosylated Asn in extra-cellular loops and the His responsible for the binding of two hemes in transmembrane α helix III and V are indicated. Mutations that lead to X^{0}CGD are localized in the transmembrane and the cytosolic tail of gp91*phox* whereas mutations causing X$^+$CGD and X$^-$CGD are positioned in the cytosolic NADPH binding site of gp91*phox*

in the encoding region of *CYBB*, one in exon 9 (c1024_1026delCTG/insT) and the other in exon 11 (c1373insT). Both mutations led to a frameshift and the introduction of a stop codon, p.Leu342TyrfsX3 and p.Gln459AlafrX26 for P13 and P17 respectively. No mutated gp91*phox* proteins could be detected by western blot or flux cytometry in the new CGD patients' neutrophils, P7, P9, P13 and P17 (X91^{0}CGD) (Table II). Unfortunately the blood samples of patients P1 and the carrier P6* came from far away, and preserving intact neutrophils for western-blot analysis was not possible. P6 was a carrier of a new nonsense mutation which always leads to a X^{0}CGD phenotype [6]. The two X$^+$CGD missense mutations in exon 10 resulting in the change of Gly408Arg and Pro415Leu in gp91*phox* have been described in the literature (for review see [3, 6]). As we previously reported [9], the nonsense mutation (c469C>T) in exon 5 of *CYBB* caused the translation of two types of gp91*phox* mRNA, one containing exon 5 with the nonsense mutation and the second with this exon skipped (data not shown). Finally, three X91^{0}CGD were caused by large deletions in the *CYBB* sequence (P19 to P21). We determined the exact size of the deletion in the *CYBB* gene for patient P19 because of the absence of exon 7 to 11 in the cDNA (Fig. 2a and e) and in the *CYBB* gene (Fig. 2b). We succeeded in amplifying and sequenced the genomic sequence of *CYBB* from the beginning of intron 6 to the beginning of intron 11 (Fig. 2c and e) for patient P19 and his mother who was a carrier, but not in the control. Indeed, we found a deletion of 8,494 bp from the end half of intron 6 to the end half of exon 11. To confirm the size of this deletion we succeeded in amplifying a 2,099 bp DNA fragment using a forward primer in exon 6 to a backward primer in intron 11 for the patient P19 and his mother only (Fig. 2d). No *CYBB* gene amplification was obtained for patients P20 and P21. Large deletions including the absence of *CYBB* was suspected and characterized by FISH (Fig. 3). Indeed, no hybridization with Texas Red labeled BAC RP11-715D15 and BAC RP11-777A16 suggested that *CYBB* and *XK* genes were absent. This was in accordance with the presence of 10 % acanthocytes in the circulating red blood of patient P20 consistent with a

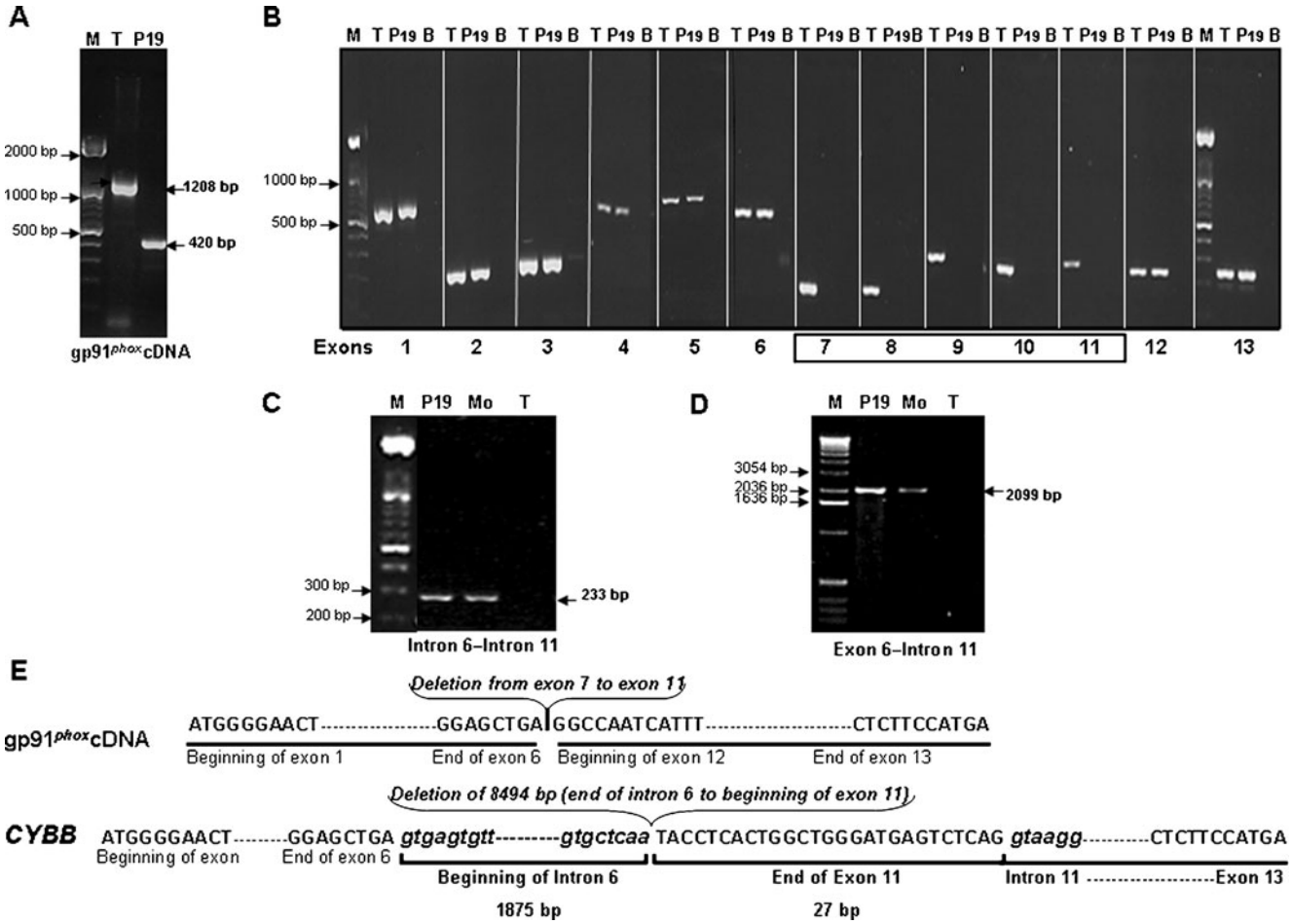

Fig. 2 Genetic analysis of cDNA and genomic DNA from patient 19. **a**. Gp91*phox* cDNA was amplified using a forward primer in exon 6 and a reverse primer in exon 12 as described in Materials and Methods. After sequencing of the 420 bp fragment of patient 19, we found a deletion from exon 7 to exon 11 as compared to the PCR amplified fragment of 1,208 bp from the control cDNA. **b**. All the exons of *CYBB* were amplified by PCR using forward and reverse primers in the flanking intronic regions of the gene. The absence of exon 7 to 11 found in gp91*phox* cDNA was confirmed in the *CYBB* gene. **c**. To find the exact size of the deletion in *CYBB*, the genomic DNA of Patient 19 was amplified by PCR using a *forward* primer localized in the beginning of intron 6 and a reverse primer in the beginning of intron 11. Amplification was only obtained for Patient 19 and in his mother (fragment of 233 bp) whereas no amplification could be obtained in the control fragment because of its large length (intron 6 to intron 11). The exact size of the deletion was determined after sequencing. **d**. We confirmed the size of the deletion by amplifying another genomic fragment of Patient 19 and his mother using a forward primer at the beginning of exon 6 and a reverse primer at the beginning of intron 11. This confirmed that his mother was a carrier for the disease. **e**. Schematic representation of the deletions found in gp91*phox* cDNA and in *CYBB* for Patient 19. Exons 7 to 11 were absent from the gp91*phox* cDNA of Patient 19. A deletion of 8,484 bp was found in the *CYBB* of this patient. This deletion is from a sequence at the end of intron 6 to a sequence in the beginning of exon 11. The AG acceptor site at the end of intron 10 was deleted in the *CYBB* gene of Patient 19

MacLeod syndrome (Table I). In addition, a diminished and no signal for P20 and P21 respectively using Texas red labelled BAC RP11-641C23 confirmed that the deleted region was shorter for patient P20 than for patient P21. However, the most centrosomal region of chromosome Xp21.1 was labelled after hybridization with BAC RP11-12J5 in both patients (data not shown). More precise information about the size of the deletion in chromosome band Xp11.4p21.1 of patients P20 and P21 was obtained using the CGH-array approach (Fig. 4). The first deletion is a 210 kb loss extending from base 37,479,113 to 37,689,027 (GRCh37/hg19) from the Xp telomere including the *LANCL3*, *XK* and *CYBB* genes (P20). The second is a 1.3 Mb deletion from base 36,449,924 to 37,787,309 (GRCh37/hg19) from the Xp telomere including the *FAM47C*, *PRRG1*, *PRGP1*, *LANCL3*, *XK*, *CYBB* and *DYNLT3* genes (P21). No other abnormalities larger than 3 probes were observed, excluding well-known benign copy number variations previously reported in DGV. The carrier status of P21's mother was confirmed by MLPA analysis whereas the mother of patient P20 was not a carrier (data not shown). Most of the mothers of the studied patients were heterozygous for the mutation (86 %) except those of patients P9, P17 and P20 (Table II). This suggests that these mutations were *de novo* mutations (Table II).

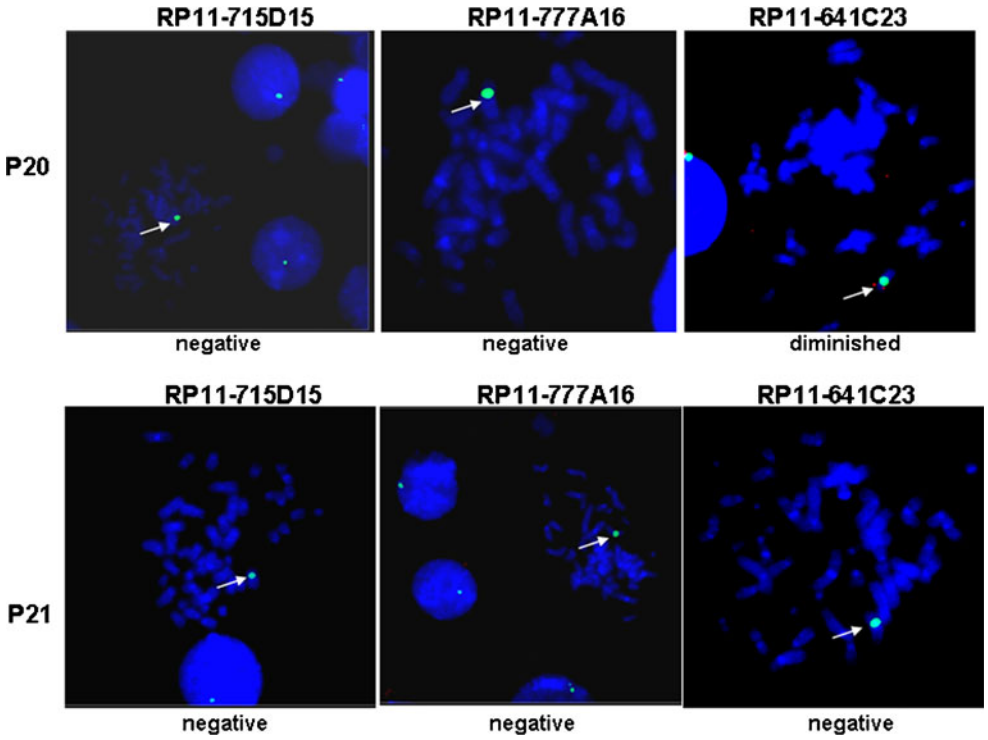

Fig. 3 Characterization of the deletions in *CYBB* from Patients 20 and 21 by Fluorescence in Situ Hybridization. Fluorescence in Situ Hybridization (FISH) studies were performed on EBV immortalized B lymphocytes from patient 20 and patient 21 as described in Material and Methods. BAC probes were selected from UCSC genome browsers and labeled by fluorescent Texas red. Slides were counterstained with DAPI/ Vectashield and FISH signals were captured with an equipped fluorescence microscope. Twenty metaphases were analysed per slide

We found 3 cases of ARCGD with mutations in *NCF1*, *NCF2* and *CYBA* genes. The AR47^{0}CGD of patient P22 was due to the classical dinucleotide deletion (ΔGT) at a GTGT repeat at the beginning of exon 2 in the *NCF1* gene. Detection of AR47^{0}CGD carriers was determined using the Gene-Scan method [21]. Then a 7-bp deletion was found at the beginning of exon 5 in *CYBA* for patient P21 as previously described [20, 26]. Finally, we found a new

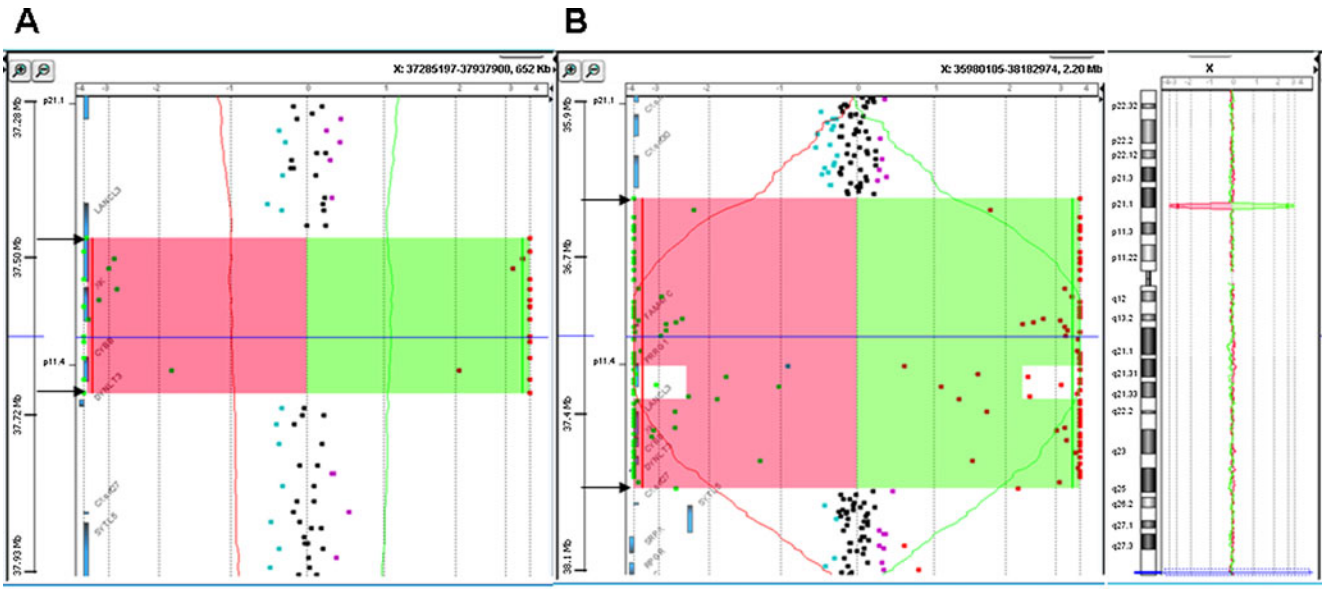

Fig. 4 CGH-array profile of the Xp11.4p21.1 region from Patients 20 and 21. **a**. The 210 Kb deletion of Patient P20 located between oligonucleotides A_16_P03689979 and A_16_P21443070 and including a part of the *LANCL3* gene, the *XK* and *CYBB* genes. **b**. The 1,3 Mb deletion in Patient P21 located between oligonucleotides A_16_P21440444 and A_14_P123289 and including the *FAM47C*, *PRRG1*, *PRGP1*, *LANCL3*, *XK*, *CYBB* and *DYNLT3* genes. Arrows indicate the breakpoints as defined by Agilent 180K. The genes located within the deleted region are shown on the right. Results are presented as signal ratio plots where each dot indicates a separate oligonucleotide. X-axis shows the log 2 ratio of signal intensity and Y-axis corresponds to the genomic position in megabases of DNA. The value of zero represents equal fluorescence intensity ratio between sample and reference DNA. Copy-number losses shift the ratio to the left (−∞). The two patients have homozygous deletions in the *CYBB* region

nonsense mutation in *NCF2* (c29G>A) that generates a stop codon at position Trp10 at the beginning of the p67*phox* sequence in the TPR1-4 region. In all the studied cases there was correlation between functional and genetic analysis data (Table II).

Discussion

Twenty-one out of 24 CGD patients in the present study presented mutations in the *CYBB gene* known to cause X-linked CGD (X91 CGD, OMIM #306400) [6]. Nonsense and missense mutations together represented 50 % of mutations, splice site mutations represented 27 % and deletions and insertions accounted for 23 %, which is not in accordance with what was found in a large study reporting 681 mutations in *CYBB* where missense and nonsense, splice site, and deletions and insertions represented 35 %, 18 % and 43 % of mutations respectively [6]. Our series is probably too small to be statistically relevant. Despite the small group of patients, we found the whole spectrum of mutations apart from promoter mutations which are extremely rare (0.6 % according to [6]). Their distribution within the *CYBB* gene also exhibited great heterogeneity. Three different mutations were found in genes involved in AR CGD forms. The first was the classical GT homozygous deletion in exon 2 of the *NCF1* gene encoding the p47*phox* protein, due to recombination events between *NCF1* and its two pseudogenes (*ΦNCF1*) that contain GT deletions [27]. The second AR mutation was a 7 base deletion in exon 5 of *CYBA* encoding p22*phox*, previously found in a patient from Tunisia and in a Jordanian family [20, 26]. A recent study reported the existence of copy number variation of the Φ*NCF1* genes in three normal populations African-American, Caucasian and Mexican [28]. This could complicate the interpretation of results from the Gene Scan method. However, patient P24 was Caucasian and we readily detected the carrier status of both his parents and one of his brothers (ratio GT/GTGT 5/1) which was different from the non-carrier relatives (another brother and his sister, ratio GT/GTGT 2/1). The last new mutation found in *NCF2* was a nonsense mutation introducing a stop codon at Trp10 in the TPR region of p67*phox*. This region interacts with the small G protein Rac2 and is involved in the regulation of the NADPH oxidase complex activity [29]. However, the resulting truncated protein was probably too short to be expressed stably.

Mutations in *CYBB* affected both coding and non-coding regions and eight of them were new. Thirteen point mutations (missense and nonsense) were widely distributed over the Nox2 sequence as seen in Fig. 1 whereas X^+ and X^- CGD mutations were particularly located in the cytosolic part of Nox2 which is the dehydrogenase domain of the enzyme [30]. The range of mutations identified in the present study spanned nearly all types of mechanisms by which genetic change can disrupt gene expression. The most common forms of mutation were single-base changes resulting in nonsense (6) or missense (6) codons. A number of mechanisms of single nucleotide substitution have been identified [31]. The best known is methylation-induced deamination of cytosine, which causes the formation of thymidine in the sense strand of DNA and a G→A substitution in the antisense strand. In our series, this type of nonsense mutation was found in 4/6 cases and, in most of these cases, the substitution is in cytidine-phosphate-guanosine dinucleotides (5′ to 3′; CpG). We report a new nonsense mutation which is a G493T substitution in exon 6 of *CYBB* (P6) leading to the introduction of a stop codon at Gly165. The G→T substitution seems to be a rare genetic event because only 16 of 96 nonsense mutations have been reported in the recently published study that included 681 X-linked CGD patients [6]. We found this mutation in an adolescent with a late presentation of clinical symptoms of CGD. Bronchoscopic examination showed diffuse fine granulomatous nodes in all airways. We found a moderate reduction of NADPH oxidase activity in her neutrophils of 30 % compared to control values (NBT test and Amplex Red, Table II), which is not in accordance with her clinical profile resembling a XCGD patient profile or a XCGD carrier with an extremely skewed X-inactivation event [32, 33]. Thus, we have no explanation for these quite severe clinical complications in this XCGD carrier. The second unusual and new result was the double missense mutation found in patient P7 leading to an $X91^0$ CGD phenotype and carried by his mother. Both mutations (c625C>G) in exon 6 and (c1510C>T) in exon 12 were new. The first one leads to the substitution His209Asp in the potential V transmembrane section of gp91*phox*. His209 is one of the four His involved in the coordination of both hemes in gp91*phox* [34]. Several other substitutions of this amino acid (Ser, Arg, Gln, and Tyr) have been previously reported [6] and one was found in patient P8 of this study (His209Tyr). The defect in incorporation of one heme in gp91*phox* probably leads to a poorly structured protein perturbing the electron transfer from the FAD to the hemes. The second missense mutation leads to a new substitution Thr503Ile in gp91*phox*. At present there is no evidence that this mutation is detrimental for the expression of gp91*phox* and NADPH oxidase activity, although Thr503 is close to the NADPH binding site of gp91*phox*. Previous evidence shows that a Leu505Arg mutation close to this stretch affects the oxidase complex activation process through alteration of p67*phox* activation of cytochrome b_{558}, thus partially affecting access of NADPH to its binding site [35]. Thr and Ile both have chiral side chains and differ only in the substitution of a hydroxyl group for a methyl group on the β carbon. However, the change from a polar amino acid to a hydrophobic one could perturb the close

environment of the NADPH binding site. To our knowledge this is only the second double mutation found in *CYBB* in an X-linked CGD patient [36]. We found two new mutations affecting correct mRNA synthesis; no gp91*phox* mRNA synthesis was detected for the mutation c45+3A>T+5delG in intron 1 (P1) and only a faint amount of gp91*phox* mRNA was found for the mutation c674+4delAGTG in intron 6 (P9) including skipping of exon 6 (data not shown) resulting in an $X91^0$ phenotype with no gp91*phox* expression, as in most previously reported splicing mutations in X-linked CGD [6]. Eight and thirteen different splice mutations were reported in the 5′intron sequence of intron 1 and intron 6 respectively but the deletion of the corresponding exon was explored only in a few of them [6]. Finally, the last two new mutations found were a deletion/insertion in exon 9 (c1024_1026delCTG/insT) and a one base insertion in exon 11 (c1373insT) both leading to a frameshift introducing a stop codon at amino acid 359 and 485 respectively (Table II). We observed reduced mRNA stability for both mutations and in both cases the mutated gp91*phox* proteins were not expressed probably because of misfolding. Deletions in the *CYBB* gene are a frequently encountered cause of X-linked CGD, but up to now no deletions have been reported in the sequence close to the c1024–1026 region. On the contrary, in *CYBB* insertions are rare genetic events and only one nonsense mutation c1375C>T has been found within this region [6]. Deletions and insertions often occur in runs of identical nucleotides because of slipped mispairing at the DNA replication fork and repeat elements of consensus sequences causing this phenomenon have been previously identified [37–39]. Unfortunately, we did not find any consensus sequences within the above deletion and insertion mutations.

At least two (P20 and P21) of the 5 deletion mutations (P1, P9, P19, P20 and P21) were large enough to affect the adjacent McLeod gene (*XK*). Both deletions were analysed by FISH as previously reported for other CGD patients and carriers [40, 41]. However, this is the first time that the actual size of large deletions in CGD (i.e. 210 kb and 1.3 Mb for P20 and P21 respectively) has been revealed by array-CGH [22] and the carrier status of these patients characterized by MLPA [23]. It is of importance to check the presence of the XK gene because when transfused, McLeod phenotype patients may respond with anti-Kx and anti-Km antibodies, rendering future transfusions extremely difficult [42]. Thirty large deletions out of 681 different mutations of CGD were reported to be associated with the *KX* gene deletion [6]. Large deletions and insertions (>50 bp) are generally considered to be caused by meiotic or mitotic recombination between chromosomes misaligned at partially homologous sequences [37].

Most of the X linked CGD patients (16/21) had at least one severe infection in vital organs such as the lungs or the liver, associated or not with granuloma. The age of diagnosis of these patients varied from 3 months to 6 years. The genetic defect in *CYBB* was very heterogeneous for the five XCGD patients presenting the mildest clinical symptoms (P11, P14, P16, P18 and P19). Indeed as seen in Table II, these patients had nonsense, missense, splice and deletion mutations. Thus, we conclude that in our patients there was no clear correlation between genotype and phenotype for CGD with mild clinical presentation. This was previously observed in other cohorts [30, 39]. However, the mild clinical presentation of P14 could be explained by the residual oxidase activity found in his neutrophils. Surprisingly the clinical manifestations of patient P6 resembled those of mild forms of CGD ($AR47^0$CGD or $X91^-$CGD), where a slight NADPH oxidase activity can be detected [8]. Indeed, CGD was suspected when she was 17-years old when generalised lymphadenopathies and non-specified granulomatous processes in both lung and in lymph nodes were found on biopsy examination. A bronchoscope examination had revealed diffuse fine granulomatous nodes in the lung leading initially to a suspicion of sarcoïdosis. A specific granulomatous process as in tuberculosis, CVID and cat scratch disease were excluded. No signs of malignancy were detected on biopsy examination of bone marrow. Eventually, the status of this patient as a CGD carrier was formally established by functional and genetic testing as described in Table II.

The $AR22^0$CGD and $AR67^0$CGD cases (who were both probands), were diagnosed very early (at 2 and 3 months respectively) and demonstrated more severe clinical profiles compared with the $AR47^0$CGD case not diagnosed until age 7 years. This confirms that cytochrome b_{558} the redox element of the NADPH oxidase complex and the cytosolic protein p67*phox* are crucial elements for NADPH oxidase activity whereas p47*phox* does not seem to participate directly in regulating the activity of the NADPH oxidase but serves to optimise protein activity. Thus, the clinical severity of the disease seems to be associated with defects in specific NADPH oxidase proteins and the extent of residual activity, but not with the type of mutation involved [8]. However, 3 months after establishment of the CGD diagnosis, the $AR47^0$CGD patient developed coronary vascularitis compatible with a Kawasaki syndrome, which is unusual in CGD. All the 24 CGD patients were treated with long-term antibiotics and antifungal drugs and 3 of them had temporary interferon γ injections. One patient died after developing an invasive aspergillosis resistant to treatment (P23). Of the five patients with sudden allogeneic BMT, one died because of an inflammatory flare up (P10). In patients with severe clinical expression of CGD, it is advocated to perform BMT as early as possible to minimise the chronic complications [43]. Gene therapy could be a promising alternative treatment strategy [44].

Finally, investigation of X-linked CGD carrier status, revealed the mutated gene and functionally abnormal phagocytes in 86 % of mothers. Although the series studied here is small, the apparent spontaneous mutation rate of about 14 % falls well below Haldane's calculation which estimated that 25–30 % of cases of X-linked disorders represent new mutations [45]. However, the examination of carrier status is of great importance for genetic counselling and prenatal diagnosis.

Acknowledgments MJS is grateful for support from the University Joseph Fourier, Faculty of Medicine; the Ministry of Education and Research, MENRT; the Regional Clinical Research Department, DRCI, Grenoble University Hospital, the CGD Research Trust grant award reference J4G/09/09 and from the National Institutes of Health Grant N01–AI-30070 from the Immunodeficiency Network and the Primary Immunodeficiency Disease Consortium.

The authors are grateful to Dr D. Roos and Dr A. J. Verhoeven for the generous gift of mAb449 and mAb48 antibodies against the two subunits of the cytochrome b_{558}. We also thank Dr Alison Foote for editing the manuscript.

References

1. Malech HL, Hickstein DD. Genetics, biology and clinical management of myeloid cell primary immune deficiencies: chronic granulomatous disease and leukocyte adhesion deficiency. Curr Opin Hematol. 2007;14:29–36.
2. Takeya R, Sumimoto H. Molecular mechanism for activation of superoxide-producing NADPH oxidases. Mol Cells. 2003;31:271–7.
3. Stasia MJ, Li XJ. Genetics and immunopathology of chronic granulomatous disease. Semin Immunopathol. 2008;30:209–35.
4. Matute JD, Arias AA, Wright NA, Wrobel I, Waterhouse CC, Li XJ, Marchal CC, Stull ND, Lewis DB, Steele M, Kellner JD, Yu W, Meroueh SO, Nauseef WM, Dinauer MC. A new genetic subgroup of chronic granulomatous disease with autosomal recessive mutations in p40phox and selective defects in neutrophil NADPH oxidase activity. Blood. 2009;114:3309–15.
5. Roos D, Kuhns DB, Maddalena A, Bustamante J, Kannengiesser C, de Boer M, van Leeuwen K, Köker MY, Wolach B, Roesler J, Malech HL, Holland SM, Gallin JI, Stasia MJ. Hematologically important mutations: the autosomal recessive forms of chronic granulomatous disease (second update). Blood Cells Mol Dis. 2010;44:291–9.
6. Roos D, Kuhns DB, Maddalena A, Roesler J, Lopez JA, Ariga T, Avcin T, de Boer M, Bustamante J, Condino-Neto A, Di Matteo G, He J, Hill HR, Holland SM, Kannengiesser C, Köker MY, Kondratenko I, van Leeuwen K, Malech HL, Marodi L, Nunoi H, Stasia MJ, Ventura AM, Witwer CT, Wolach B, Gallin JI. Hematologically important mutations: X-linked chronic granulomatous disease (third update). Blood Cells Mol Dis. 2010;1545:246–65.
7. Van den Berg JM, van Koppen E, Ahlin A, Belohradsky BH, Bernatowska E, Corbeel L, Español T, Fischer A, Kurenko-Deptuch M, Mouy R, Petropoulou T, Roesler J, Seger R, Stasia MJ, Valerius NH, Weening RS, Wolach B, Roos D, Kuijpers TW. Chronic granulomatous disease: the European experience. PLoS One. 2009;4:e5234.
8. Kuhns DB, Alvord WG, Heller T, Feld JJ, Pike KM, Marciano BE, Uzel G, DeRavin SS, Long Priel DA, Soule BP, Zarember KA, Malech HL, Holland SM, Gallin JI. Residual NADPH oxidase and survival in chronic granulomatous disease. N Engl J Med. 2010;363:2600–10.
9. Stasia MJ, Bordigoni P, Floret D, Brion JP, Bost-Bru C, Michel G, Gatel P, Durant-Vital D, Voelckel MA, Li XJ, Guillot M, Maquet E, Martel C, Morel F. Characterization of six novel mutations in the *CYBB* gene leading to different sub-types of X-linked chronic granulomatous disease. Hum Genet. 2005;116:72–82.
10. Böyum A. Isolation of mononuclear cells and granulocytes from human blood. Scand J Clin Lab Investig. 1968;21:77–89.
11. Cohen-Tanugi L, Morel F, Pilloud-Dagher MC, Seigneurin JM, François P, Bost M, Vignais PV. Activation of O_2^- generating oxidase in heterologous cell-free system derived from Epstein-Barr-virus-transformed human B lymphocytes and bovine neutrophils. Eur J Biochem. 1991;202:649–55.
12. Stasia MJ, Brion JP, Martel C, Morel F. Severe clinical forms of cytochrome *b*-negative chronic granulomatous disease (X91$^-$) in three children with a point mutation in the promoter region of the *CYBB* gene. J Infect Dis. 2003;188:1597–604.
13. Carrichon L, Picciocchi A, Debeurme F, Defendi F, Beaumel S, Jesaitis AJ, Dagher MC, Stasia MJ. Characterization of superoxide overproduction by the D-Loop(Nox4)-Nox2 cytochrome b(558) in phagocytes-differential sensitivity to calcium and phosphorylation events. Biochim Biophys Acta. 2011;1808:78–90.
14. Zhou M, Diwu Z, Panchuk-Voloshina N, Haugland RP. A stable nonfluorescent derivative of resorufin for the fluorometric determination of trace hydrogen peroxide: applications in detecting the activity of phagocyte NADPH oxidase and other oxidases. Anal Biochem. 1977;253:162–8.
15. Picciocchi A, Debeurme F, Beaumel S, Dagher MC, Grunwald D, Jesaitis AJ, Stasia MJ. Role of the putative second transmembrane region 45LLGSALALARAPAACLNFNCMLILL69 of Nox2 in its structural stability and electron transfer in the phagocytic NADPH oxidase. J Biol Chem. 2011;286:28357–69.
16. Laemmli UK. Cleavage of structural proteins during the assembly of the head of bacteriophage T4. Nature. 1970;227:680–5.
17. Towbin H, Staehelin T, Gordon J. Electrophoretic transfer of proteins from polyacrylamide gels to nitrocellulose sheets: procedure and some application. Proc Natl Acad Sci USA. 1979;76:4350–435.
18. Verhoeven AJ, Bolscher GJM, Meerhof L, van Zwieten R, Keijer J, Weening RS, Roos. Characterization of two monoclonal antibodies against cytochrome b_{558} of human neutrophils. Blood. 1989;73:1686–94.
19. Vergnaud S, Paclet MH, El Benna J, Pocidalo MA, Morel F. Complementation of NADPH oxidase in p67-phox/p40-phox interaction. Eur J Biochem. 2000;267:1059–67.
20. Bakri F, Martel C, Khuri-Bulos N, Mahafzah A, El-Khateeb MS, Al-Wahadneh AD, Hayajneh WA, Hamamy HA, Maquet E, Molin M, Stasia MJ. First report of clinical, functional, and molecular investigation of chronic granulomatous disease in nine Jordanian families. J Clin Immunol. 2009;29:215–30.
21. Dekker J, de Boer M, Roos D. Gene-scan method for the recognition of carriers and patients with p47*phox*-deficient autosomal recessive chronic granulomatous disease. Exp Hematol. 2001;29:1319–25.
22. Menten B, Maas N, Thienpont B, Buysse K, Vandesompele J, Melotte C, de Ravel T, Van Vooren S, Balikova I, Backx L, Janssens S, De Paepe A, De Moor B, Moreau Y, Marynen P, Fryns JP, Mortier G, Devriendt K, Speleman F, Vermeesch JR. Emerging patterns of cryptic chromosomal imbalance in patients with idiopathic mental retardation and multiple congenital anomalies: a new series of 140 patients and review of published reports. J Med Genet. 2006;43:625–33.
23. Coutton C, Monnier N, Rendu J, Lunardi J. Development of a multiplex ligation-dependent probe amplification (MLPA) assay

for quantification of the OCRL1 gene. Clin Biochem. 2010;43:609–14.
24. Bradford MM. A rapid and sensitive method for quantitation of microgram quantities of protein utilizing the principle of protein-dye binding. Anal Biochem. 1976;72:248–54.
25. Araujo A, Pagnier A, Frange P, Wroblewski I, Stasia MJ, Morand P, Plantaz D. Lymphohistiocytic activation syndrome and Burkholderia cepacia complex infection in a child revealing chronic granulomatous disease and chromosomal integration of the HHV-6 genome. Arch Pediatr. 2011;18:416–9.
26. El Kares R, Barbouche MR, Elloumi-Zghal H, Bejaoui M, Chemli J, Mellouli F, Tebib N, Abdelmoula MS, Boukthir S, Fitouri Z, M'Rad S, Bouslama K, Touiri H, Abdelhak S, Dellagi MK. Genetic and mutational heterogeneity of autosomal recessive chronic granulomatous disease in Tunisia. J Hum Genet. 2006;51:887–95.
27. Noack D, Rae J, Cross AR, Ellis BA, Newburger PE, Curnutte JT, Heyworth PG. Autosomal recessive chronic granulomatous disease caused by defects in NCF-1, the gene encoding the phagocyte p47-phox: mutations not arising in the NCF-1 pseudogenes. Blood. 2001;97:305–11.
28. Brunson T, Wang Q, Chambers I, Song Q. A copy number variation in human NCF1 and its pseudogenes. BMC Genet. 2010;11–3.
29. Nisimoto Y, Freeman JL, Motalebi SA, Hirshberg M, Lambeth JD. Rac binding to p67(phox). Structural basis for interactions of the Rac1 effector region and insert region with components of the respiratory burst oxidase. J Biol Chem. 1997;272:18834–41.
30. Debeurme F, Picciocchi A, Dagher MC, Grunwald D, Beaumel S, Fieschi F, Stasia MJ. Regulation of NADPH oxidase activity in phagocytes: relationship between FAD/NADPH binding and oxidase complex assembly. J Biol Chem. 2010;285:33197–208.
31. Cooper DN, Krawczak M. The mutational spectrum of single base-pair substitutions causing human genetic disease:patterns and predictions. Hum Genet. 1990;85:55–74.
32. Wolach B, Scharf Y, Gavrieli R, de Boer M, Roos D. Unusual late presentation of X-linked chronic granulomatous disease in an adult female with a somatic mosaic for a novel mutation in *CYBB*. Blood. 2005;105:61–6.
33. Lewis EM, Singla M, Sergrant S, Koty PP, McPhail LC. X-linked chronic granulomatous diseasesecondary to skewed X chromosome inactivation in a female with a novel CYBB mutation and late presentation. Clin Immunol. 2008;129:372–80.
34. Henderson LM. Role of histidines identified by mutagenesis in the NADPH oxidase-associated H+ channel. J Biol Chem. 1998;273:33216–23.
35. Li XJ, Fieschi F, Paclet MH, Grunwald D, Campion Y, Gaudin P, Morel F, Stasia MJ. Leu505 of Nox2 is crucial for optimal p67phox-dependent activation of the flavocytochrome b558 during phagocytic NADPH oxidase assembly. J Leukoc Biol. 2007;81:238–49.
36. Stasia MJ, Lardy B, Maturana A, Rousseau P, Martel C, Bordigoni P, Demaurex N, Morel F. Molecular and functional characterization of a new X-linked chronic granulomatous disease variant ($X91^{+}$) case with a double missense mutation in the gp91-phox-cytosolique C-terminal tail. Biochem Biophys Acta. 2002;1586:316–30.
37. Krawczak M, Cooper DN. Gene deletions causing human genetic disease: mechanisms of mutagenesis and the role of the local DNA sequence environment. Hum Genet. 1991;86:425–41.
38. Cooper DN, Krawczak M. Mechanisms of insertional mutagenesis in human genes causing genetic disease. Hum Genet. 1991;87:409–15.
39. Krawczak M, Reiss J, Cooper DN. The mutational spectrum of single base-pair substitutions in mRNA splice junctions of human genes: causes and consequences. Hum Genet. 1992;90:41–54.
40. Simon KC, Noack D, Rae J, Curnutte J, Sarraf S, Kolev V, Blancato JK. Long polymerase chain reaction-based fluorescence in situ hybridization analysis of female carriers of X-linked chronic granulomatous disease deletions. J Mol Diagn. 2005;7:183–6.
41. Di Matteo G, Giordani L, Finocchi A, Ventura A, Chiriaco M, Blancato J, Sinibaldi C, Plebani A, Soresina A, Pignata C, Dellepiane RM, Trizzino A, Cossu F, Rondelli R, Rossi P, De Mattia D, Martire B, IPINET (Italian Network for Primary Immunodeficiencies). Molecular characterization of a large cohort of patients with chronic granulomatous disease and identification of novel CYBB mutations: an Italian multicenter study. Mol Immunol. 2009;46:1935–41.
42. Redman CM, Marsh WL. The Kell blood group system and the McLeod phenotype. Semin Hematol. 1993;30:209–18.
43. Martinez CA, Shah S, Shearer WT, Rosenblatt HM, Paul ME, Chinen J, Leung KS, Kennedy-Nasser A, Brenner MK, Heslop HE, Liu H, Wu MF, Hanson IC, Krance RA. Excellent survival after sibling or unrelated donor stem cell transplantation for chronic granulomatous disease. J Allergy Clin Immunol. 2012;129:176–83.
44. Grez M, Reichenbach J, Schwäble J, Seger R, Dinauer MC, Thrasher AJ. Gene therapy of chronic granulomatous disease: the engraftment dilemma. Mol Ther. 2011;19:28–35.
45. Haldane JBS. The ratio of spontaneous mutation of a human gene. J Genet. 1935;31:317–26.
46. Den Dunnen JT, Antonarakis SE. Mutation nomenclature extensions and suggestions to describe complex mutations: a discussion. Hum Mut. 2000;15:7–12.